Appl. Phys. A 57, 291–298 (1993)

Applied Physics A Solids and Surfaces

The Influence of the "Hot"-Dimer Adsorption Mechanism on the Kinetics of a Monomer-Dimer Surface Reaction

V. D. Pereyra[1,*], **E. V. Albano**[2]

[1] Institut für Physik, Johannes Gutenberg Universität Mainz, Postfach 3980, Staudinger Weg 7, D-55128 Mainz, Germany
[2] Inifta-Universidad Nacional de la Plata, C.C. 16, Sucursal 4, (1900) La Plata, Argentina

Received 1 December 1992/Accepted 10 March 1993

Abstract. "Hot" dimers are molecules which after adsorption dissociate and each of the remaining "hot" monomers fly apart up to a maximum distance R from the original adsorption site. The influence of the "hot"-dimer adsorption mechanism on relevant aspects of the bimolecular catalyzed reaction of the type $A+(1/2)B_2(\text{"hot"}) \rightarrow AB$ is studied by means of the Monte-Carlo simulation technique. The temporal evolution of both the reactant's coverages as well as the rate of AB-production is evaluated and discussed. Due to the enhanced probability of "hot" species for encounters with other adsorbed particles, the rate of AB-production becomes faster when increasing R. This behavior may be relevant in the dynamic of some catalyzed reactions such as for example the oxidation of carbon monoxide on transition metal surfaces, i.e. $A \equiv CO$, $B_2 \equiv O_2$, and $AB \equiv CO_2$. Also the sticking coefficient of "hot" dimers and the average distance traveled by the "hot" monomers are evaluated and discussed.

PACS: 82.20.–w, 82.65.Jv, 68.10.Jy

Heterogeneously catalyzed processes involve various steps such as adsorption, surface diffusion, chemical reaction, desorption, etc. [1–3]. These processes have largely been studied by means of a great number of experimental techniques [1–3] as well as using different theoretical approaches such as, for example, mean field theories [4, 5] and computer simulations of microscopic models (see, e.g. [6–16] and references therein). Monte-Carlo simulation of reactions involving dimers are in most cases performed assuming that these species dissociate upon adsorption on the impingement sites [5, 7, 8, 10–16] and, eventually, surface diffusion of the resulting monomers is considered [5, 12].

In a very recent work Ertl et al., [17] have nicely demonstrated, by means of scanning tunneling microscopy (STM) observations, that oxygen molecules striking the Al(111) surface not only dissociate upon adsorption but also they dissipate part of their excess energy in degrees of freedom parallel to the surface. Therefore, after chemisorption of these "hot" species, the resulting oxygen atoms (monomers) fly apart, on the average, up to a distance of at least 80 Å from the original impingement site, before being accommodated on their respective adsorption sites. After this ballistic flight oxygen atoms remain practically immobile at 300 K as judged by STM images [17]. Furthermore, it is estimated that each oxygen would exhibit an initial velocity of about 6.5×10^3 m/s, traveling the distance of 40 Å within about 1 ps [17].

In view of this interesting new finding, the aim of the present work is to study, by means of the Monte-Carlo simulation technique, the influence of the "hot"-dimer adsorption mechanism on the kinetics of a monomer–dimer reaction of the type:

$$A(a) + (1/2)B_2(a, \text{"hot"}) \rightarrow AB(g) + 2(^*)\,, \qquad (1)$$

where $(^*)$, (a), and (g) refer to an empty site on the surface, the adsorbed and the gas phase, respectively. Note that the reaction scheme of (1) mimics the oxidation of carbon monoxide on transition metal surfaces, i.e. $A \equiv CO$, $B_2 \equiv O_2$, and $AB \equiv CO_2$, which has largely been studied ([7, 8, 10–16] and refererences therein).

In the present study we start with a lattice precovered with A-species which is exposed to a reservoir of B_2-species. Hence, the evolution of the reactant's coverages, the kinetics of AB-production, the sticking coefficient of dimers as well as the mean free path of the "hot" monomers resulting from B_2-dissociation are analyzed and discussed.

Finally, let us note that the transient mobility caused by the inability to instantaneously dissipate the energy gained by a particle after formation of the surface bond seems to be a common process in nature. In fact, surface hopping of "hot" adatoms resulting from dimer dissociation has also been considered in models for the chemisorption of nitrogen on the (100) face of tungsten [18, 19]. Also, the influence of the "hot"-dimer adsorption mechanism, in the catalyzed reaction $H_2(\text{hot}) + (1/2)O_2 \rightarrow H_2O$ on polycrystalline Pt, has been analyzed by means of a mean-field approach in the early works of Harris et al. [20]. Furthermore, the formation

* *Permanent address:* INTEQUI-Universidad Nacional de San Luis, Chacabuco y Pedernera, (5700) S. Luis, Argentina

of metastable ordered structures upon oxygen adsorption on Pd(100) ([21–23] and references therein) has also been understood assuming "hot"-O_2 dissociation, where probably the distance traveled by the monomers is rather short, namely few lattice units, in contrast to O_2/Al(111), where such distance is of the order of 40 Å [17]. On the other hand, one has to recognize the lack of conclusive experimental evidence of long range flights of O monomers on good CO-oxidation catalysts such as Pt and Pd.

The manuscript is organized as follows. In Sect. 1, the model and the Monte-Carlo simulation technique are discussed in detail. Section 2 is devoted to the presentation and discussion of the results and the conclusions and final remarks are stated in Sect. 3.

1 Description of the Model and the Simulation Technique

Simulations are performed on the square lattice of side $L=400$ assuming periodic boundary conditions. Simulations always start with lattices precovered, at random, with a certain initial concentration of A-monomers given by θ_{A_0}. Then the surface is exposed to a reservoir containing B_2-dimers.

The adsorption-reaction algorithm is the following: i) a surface site (say, site 1) is selected at random. If site 1 is already occupied the trial ends, i.e. dimer adsorption can not take place. Otherwise, if site 1 is empty, then a nearest neighbor (nn) site (say, site 2) is also selected at random. If site 2 is occupied the trial ends because, again, there is not place for dimer adsorption. But if site 2 is empty a dimer is adsorbed on the surface. ii) After deposition both monomers resulting from the dissociation of the "hot" dimer undergo a ballistic flight up to a maximum distance R measured from the initial adsorption site. Note that R is the only parameter of the model. The flight is assumed to be parallel to the axis of the "hot" dimer upon adsorption. iii) If during the flight a B-monomer hits another B-particle or ensemble of B-species which are already at rest, the flying monomer is frozen in at the collision point. This assumption is supported by the fact that one should expect a high efficiency for energy transfer and, as consequence, a high probability that these particles stick together [17]. Also, the formation of oxygen islands suggests the operation of net attractive forces between O atoms adsorbed on nn sites [17]. Otherwise, if during the flight a B-monomer hits an A-monomer we assume that the formation of an AB-species take place according to (1). This species becomes desorbed leaving two empty sites on the surface.

The Monte-Carlo time unit (t) is defined such as each site of the lattice would be visited once, in the average, i.e. $t=1$ involves $L\times L$ trials. During the adsorption-reaction process the following quantities are measured: i) the surface coverage of A- and B-species given by θ_A and θ_B, respectively; ii) the rate of AB-production (R_{AB}); iii) the sticking coefficient (S) of B_2-dimers, defined as the ratio between the number of successful adsorption attempts and the total number of attempts; and iv) the average mean free path (MFP) of the "hot" monomers, i.e. the average distance traveled by a monomer from the adsorption site up to the site where it becomes immobilly adsorbed or eventually reacts with an A-species. In order to obtain satisfactory statistics, all quantities are averaged over 10^3 different samples.

2 Results and Discussion

For the sake of clarity in the presentation of the results this section has been organized as follows. First, we discuss results obtained starting with half of the lattice precovered with A-monomers, i.e. $\theta_{A_0}=0.5$, and different choices of R; then we perform a similar study, but with $\theta_{A_0}=0.8$; and finally, we keep $R=25$ constant and use different initial coverages of A-species.

2.1 Results for $\theta_{A_0}=0.5$ and Different Choices of R

2.1.1 The Coverage with the Reactants. Figures 1 and 2 show the dependence of θ_A and θ_B on t, for different choices of R, respectively. From Fig. 1 it follows that A-species are slowly removed from the surface for the case of "cold" dimers, i.e. $R=0$. In fact, for $t=5$ one still has a small amount of A-species on the surface. The removal of A-species is considerably enhanced when the sample is

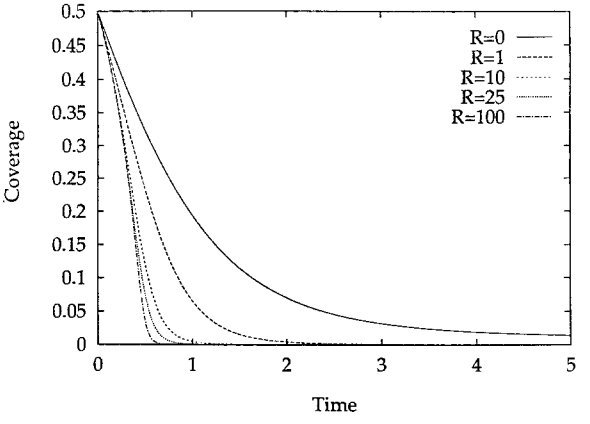

Fig. 1. Plot of the surface coverage of A-species vs the Monte-Carlo time for different choices of R, as indicated in the figure. Results are averaged over 10^3 different samples with $\theta_{A_0}=0.5$ and lattice of side $L=400$

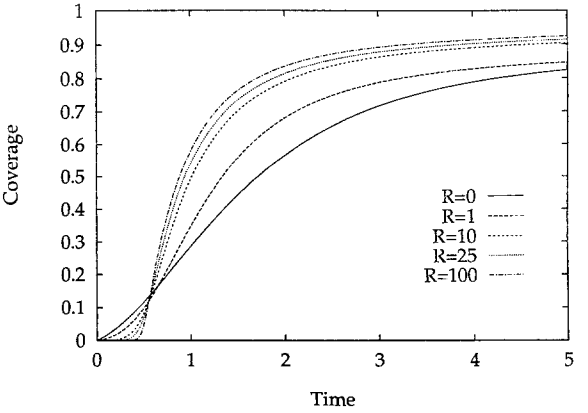

Fig. 2. Plots of the surface coverage of B-species vs time for different values of R as indicated in the figure

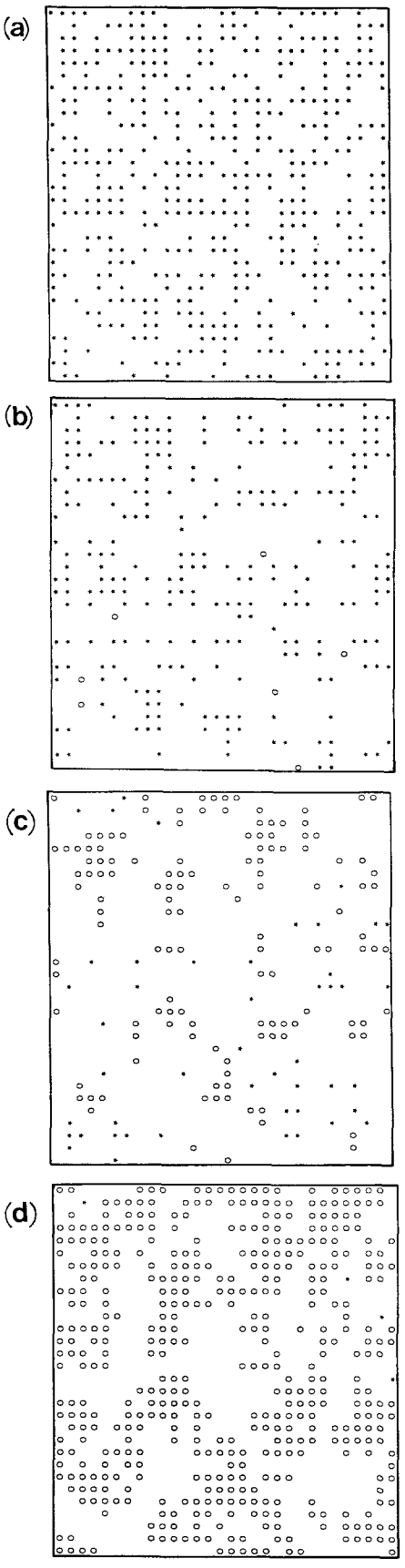

Fig. 3a–d. Snapshot configurations of the reactants on the surface taken for the same initial distribution of A-species with $\theta_{A_0}=0.5$, $R=10$ and different times. (∗) and (○) correspond to A and B-species, respectively; empty sites are left in white. **a** $t=0$; **b** $t=0.3$; **c** $t=0.6$; and **d** $t=1.0$

exposed to "hot" dimers. In fact, this effect is remarkable even for $R=1$ (see Fig. 1). After further increasing R, say, for $R=100$, one has that, roughly at $t\cong 0.5$, almost all A-species have already been annihilated (Fig. 1).

Focusing new our attention to Fig. 2, one has that, for $R=0$, θ_B increases almost linearly at early times before approaching saturation. This behavior differs from that observed using $1\leqq R\leqq 100$. In fact, due to the enhanced efficiency of "hot" dimers for encounters with A-species, at early times (say, $t<0.2$) nearly all adsorbed dimers react and therefore one has $\theta_B\cong 0$. Roughly at $t\cong 0.5$, most A-monomers have been removed (Fig. 1) and therefore θ_B grows suddenly, approaching saturation. In spite of the fact that for $t=5$ the surface is not fully saturated with B-species, Fig. 2 suggests that the asymptotic saturation value in the $t\to\infty$ limit, i.e. the so-called jamming coverage θ_j, would depend on R. This topic has been analyzed in details in a study of the adsorption kinetics of "hot" dimers [24], and, in fact, one observes that the larger R, the higher θ_j. Nevertheless, even in the $R\to\infty$ limit, there are still single vacant sites on the surface which can not be occupied by dimers.

Figure 3a–d show snapshot configurations of the reactants on the surface taken for the same initial distribution of A-species with $\theta_{A_0}=0.5$, and assuming $R=10$. Figure 3a corresponds to the surface initially precovered with A-species at $t=0$. For $t=0.3$ (Fig. 3b), a considerable amount of A-species has been removed from the surface and only few B-monomers have not reacted and are adsorbed. This snapshot shows qualitatively the high efficiency of "hot" dimers for encounters and subsequent reaction with A-species. Increasing the time by a factor of two (Fig. 3c, $t=0.6$) most A-species have already been removed and the onset of growth of B-islands is observed. Finally, at $t=1$ (Fig. 3d) B-species are the majority on the surface.

2.1.2 The Rate of AB-Production. Figure 4 shows plots of R_{AB} versus t for different choices of R ($0\leqq R\leqq 100$). For $R=0$ the maximum value $R_{AB}\cong 0.38$ is obtained in the limit $t\to 0$ and then this quantity decreases monotonically. In contrast, for $R>0$ one observes that R_{AB} exhibits peaks close to $t\cong 0.4$ and that the maximum of R_{AB} depends on R (see Fig. 4). Also, for $R>0$ one has $R_{AB}\cong 0.5$ for $t\to 0$

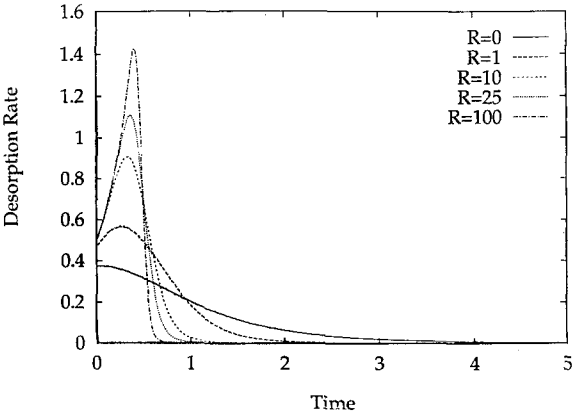

Fig. 4. Plots of the desorption rate of the AB-product as a function of time for different choices of R, as indicated in the figure. In all cases one has $\theta_{A_0}=0.5$

in agreement with the fact that at early times nearly all successful adsorption events are followed by reaction, as it is also evident in Fig. 2, where $\theta_B \cong 0$ in the $t \to 0$ limit.

From Fig. 4 it also follows that, due to the higher probability of "hot" monomers for encounters with A-species, the kinetics of the reaction process becomes substantially enhanced. This effect is more notable when increasing R (see Fig. 4) where an enhancement of about a factor 4 is obtained when comparing the curves corresponding to $R=0$ and $R=100$, respectively. Therefore, A-species becomes removed from the surface with a higher rate, as R is increased. Obviously, this result reflects the importance of the "hot"-dimer adsorption mechanism in the dynamic of catalyzed reactions.

2.1.3 The Sticking Coefficient of B_2-species. In order to study the dependence of S on both t and the total coverage $(\theta_A+\theta_B)$, it is convenient to normalize the data with respect to the sticking coefficient (S_R) that one may expect if all the adsorbed particles would be distributed at random on the surface. Since dimer adsorption requires two nn sites one has

$$S_R = (1-\theta_A-\theta_B)^2 . \tag{2}$$

Figure 5a shows plots of S/S_R versus t for different choices of R $(1 \leqq R \leqq 100)$. At early times (say, $t<0.5$) S/S_R is close to unity. This result reflects the fact that one starts to adsorb B_2-species on a randomly precovered surface with A-monomers. For $t>0.5$ and $R \leqq 10$ all A-species have already been removed from the surface (see Fig. 1) and consequently S/S_R differs from unity and strongly depends on R as evidenced in Fig. 5a. The peak of S/S_R, close to $t \cong 1.5$, is characteristic of the kinetics of B_2-adsorption only and it is not related at all to the $A+B$ reaction process since A-species are not longer adsorbed on the surface. This latter process has also been studied in detail [24].

It is also interesting to study the dependence of S on the total surface coverage $(\theta_A+\theta_B)$, as it is shown in Fig. 5b. Typically, curves start close to $\theta_A+\theta_B \cong \theta_A \cong 0.5$ and $S \cong 0.25$, since $\theta_A=0.5$ for $t=0$. B_2-adsorption followed by quick reaction with A-species (see Fig. 4) causes the total coverage to decrease and, consequently, S increases. The arrows in Fig. 5b indicate the "time direction". S reaches a maximum when the total coverage is minimum and then drops almost linearly to $S \to 0$ for $\theta_B \to \theta_B^J$, where θ_B^J is the jamming coverage with B-species (see Fig. 5b).

2.1.4 The Mean Free Path of the "Hot" Monomers. Figure 6a shows plots of the MFP/R versus t for different choices of R. In the $t \to 0$ limit MFP/R is very small (except for $R=1$, where MFP/$R \cong 0.5$) due to the quick reaction between "hot" monomers and preadsorbed A-species. When A-species start to be removed from the surface, "hot" monomers can fly more freely on the surface and the MFP

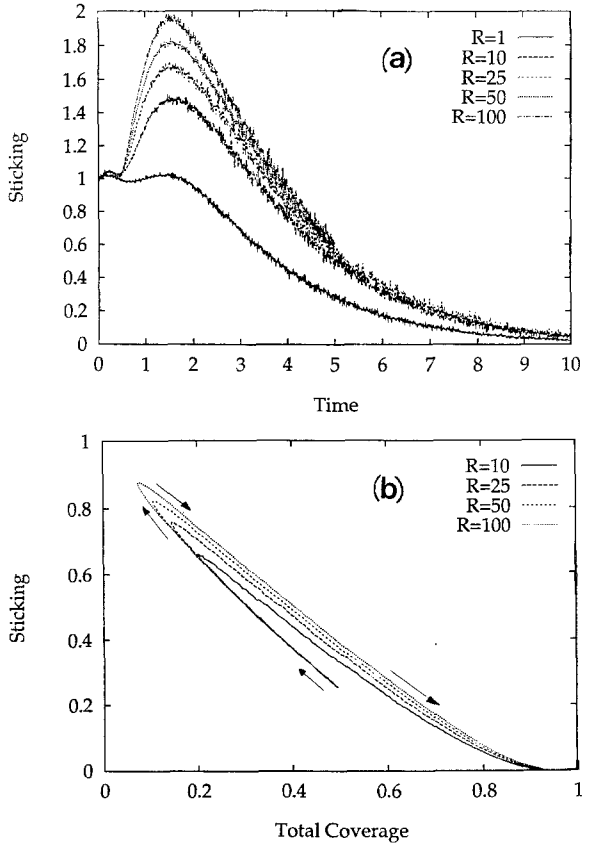

Fig. 5a, b. Plots of the sticking coefficient of "hot" dimers. **a** S/S_R vs time and **b** S vs the total coverage, respectively, for different choices of R as indicated in the figures. The *arrows* in **b** indicate the time direction. More details in the text

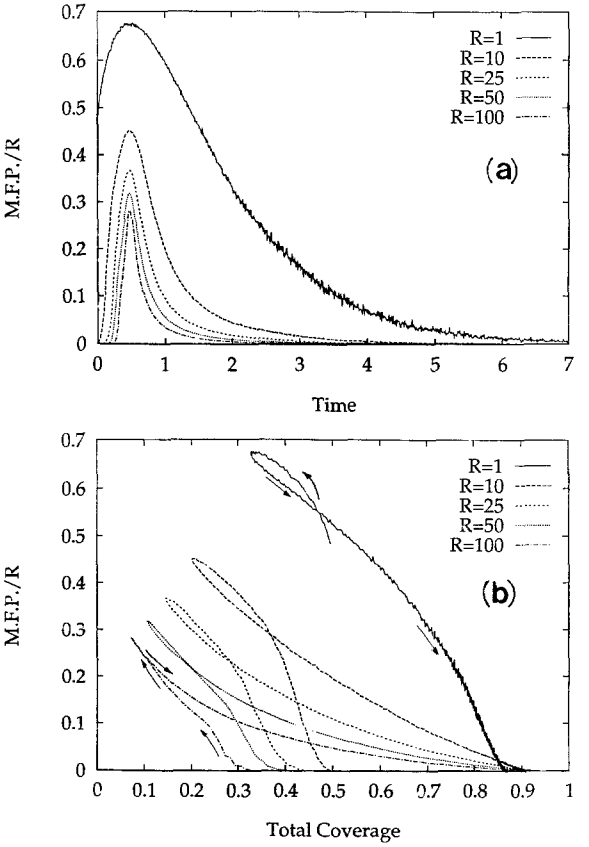

Fig. 6a, b. Plot of the average MFP of the "hot" monomers normalized with respect to R vs: **a** time and **b** total surface coverage. In all cases one has $\theta_{A_0}=0.5$. Different choices of R are indicated in the figures. *Arrows* in **b** show the time direction

increases and reaches a peak close to $t \cong 0.5$. The maximum flying efficiency corresponds to the shortest flight ($R=1$), and accounts only for 70% of the expected flight length. This efficiency markedly decreases when R is increased, and for $R=100$ one has that, in the average, "hot" monomers are able to fly, in the best case, only a distance of about $0.25\,R$. For $t>0.5$ when almost all A-species have been removed (see Fig. 1), the MFP drops because the surface becomes covered by B-species (see Fig. 2). The dependence of MFP/R on the total coverage is shown in Fig. 6b). The curves start close to $\theta_A+\theta_B \cong \theta_{A_0}=0.5$ and the arrows shown the time direction. As expected from Fig. 6a) the MFP/R reaches a maximum and then drops to MFP/$R \to 0$ as $\theta_A+\theta_B \cong \theta_B \to \theta_B^J$. It is interesting to note that the position of the maxima, given by the turning points in Fig. 6b), depends almost linearly on the total coverage.

2.2 Results for $\theta_{A_0}=0.8$ and Different Choices of R

2.2.1 The Coverage with the Reactants. Figure 7 shows the dependence of θ_A on t for three different values of R. Due to the fact that $\theta_{A_0}=0.8$ is close to the jamming coverage of the random dimer filling problem, i.e. $\theta_J \cong 0.907$ [25, 26], one has that the adsorption probability of B_2-species is strongly reduced at early times. Consequently the rate of A-removal from the surface is slower than in the previous example where $\theta_{A_0}=0.5$ (see Fig. 1). Due to this effect, the shape of the curves is different, but again "hot" dimers with larger R values are more efficient to remove A-species from the surface.

Figure 8 shows plots of θ_B versus t for the same choices of R than in Fig. 7. For $t<0.5$ and even for the smaller R value ($R=1$) one has that $\theta_B \cong 0$ because nearly all adsorption events lead to successful reactions. For $t>0.5$ one observes that θ_B increases slowly and when all monomers of type A have been removed ($t \cong 2$ for $R>1$) θ_B approaches the jamming coverage.

2.2.2 The Rate of AB-Production. Figure 9 shows the dependence of R_{AB} on t for three choices of R. As in the previous case ($\theta_{A_0}=0.5$, Fig. 4), R_{AB} exhibits a peak, but now it is considerably shifted toward later times; say, at $t \cong 1.5$, almost independent on R for $\theta_{A_0}=0.8$ in contrast to $t \cong 0.5$ for $\theta_{A_0} \cong 0.5$. One also observes an enhancement of the rate of AB-production when R is increased in agreement with the fact that "hot" species have higher probability for encounters with other adsorbed particles.

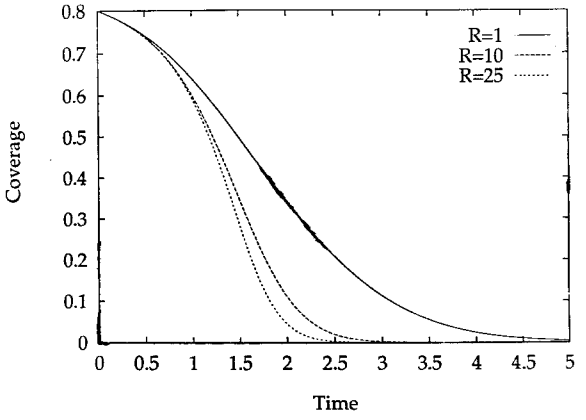

Fig. 7. Plot of the surface coverage of A-species vs the Monte-Carlo time for different choices of R, as indicated in the figure. Results are averaged over 10^3 different samples with $\theta_{A_0}=0.8$ and lattices of side $L=400$

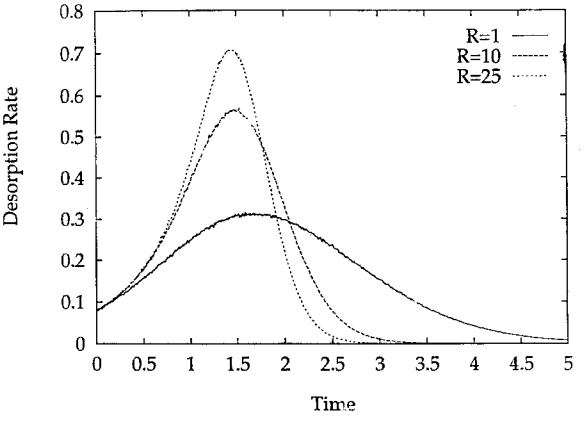

Fig. 9. Plots of the desorption rate of the AB-product as a function of time for different choices of R, as indicated in the figure. In all cases one has $\theta_{A_0}=0.8$

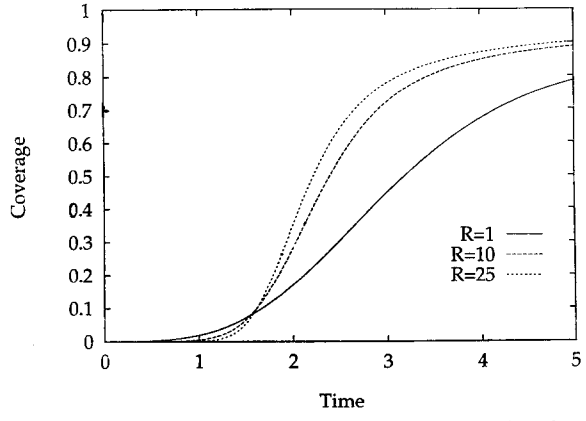

Fig. 8. Plots of the surface coverage of B-species vs time for different values of R as indicated in the figure

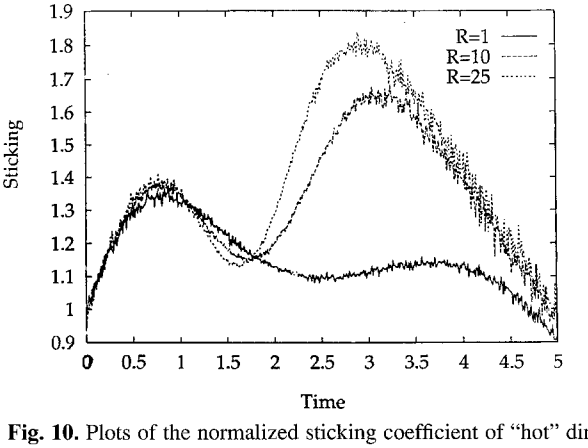

Fig. 10. Plots of the normalized sticking coefficient of "hot" dimers vs time for different choices of R as indicated in the figure, and $\theta_{A_0}=0.8$

2.2.3 The Sticking Coefficient of B_2-Species. Figure 10 shows plots of S/S_R versus t for three choices of R. These plots exhibit two different regimes, one for $t<1.5$ and the other for $t>1.5$, respectively. The first regime is dominated by the adsorption-reaction process and the curves are almost independent of R. The second regime, for $t>1.5$, is dominated by the kinetics of B_2-adsorption since A-monomers are the minority species. Note that the structure of the curves of Fig. 10 is essentially similar to that of the previous case ($\theta_{A_0}=0.5$, Fig. 5a). Nevertheless, in the latter case one has only incipient peaks at early times, but in contrast, these peaks are fully developed in the former case.

2.2.4 The Mean Free Path of the "Hot" Monomers. Figure 11a shows plots of the MFP/R versus t for different choices of the parameter R. In the $t \to 0$ limit has MFR/$R \to 0$ since the surface is highly covered with A-species and most B-monomers react immediately after adsorption. When A-species begin to be removed from the surface the MFP/R increases and reaches a maximum close to $t \cong 1.5$. The magnitude of the maximum depends on R and likewise that in the case of Fig. 6a one has that the flight of the "hot" monomers with larger R values are more restricted than that of such monomers which have smaller R values. Furthermore, the position of the peaks close to $t \cong 0.5$ for the previous case ($\theta_{a_0}=0.5$, Fig. 6a) becomes markedly shifted towards $t \cong 1.5$ when the pre-coverage with A-species is increased up to $\theta_{A_0}=0.8$ (Fig. 10a). The effect reflects the fact that more time is necessary to remove higher pre-coverages of A-species.

Figure 11b shows plots of the MFP/R versus the total surface coverage. The curves start close to $\theta_A+\theta_B \cong 0.8$ with MFR/$R \to 0$ (the arrows shown the time direction). Due to the reaction between A- and B-species the total coverage decreases and, consequently, the MFP/R increases reaching a maximum (see also Fig. 11a). The subsequent annihilation of A-species and the increasing coverage with B-species causes the MFP/R to decrease close to zero when θ_B approaches the jamming coverage.

2.3 Results for $R=25$ and Different Choices of θ_{A_0}

2.3.1 The Coverage with the Reactants. Figures 12 and 13 show the dependence of both θ_A and θ_B on t for $R=25$ and $0.1 \leqq \theta_{A_0} \leqq 0.8$, respectively. As expected, the time required in order to remove all A-species from the surface increases, almost linearly, with the initial coverage θ_{A_0} (Fig. 12). Also,

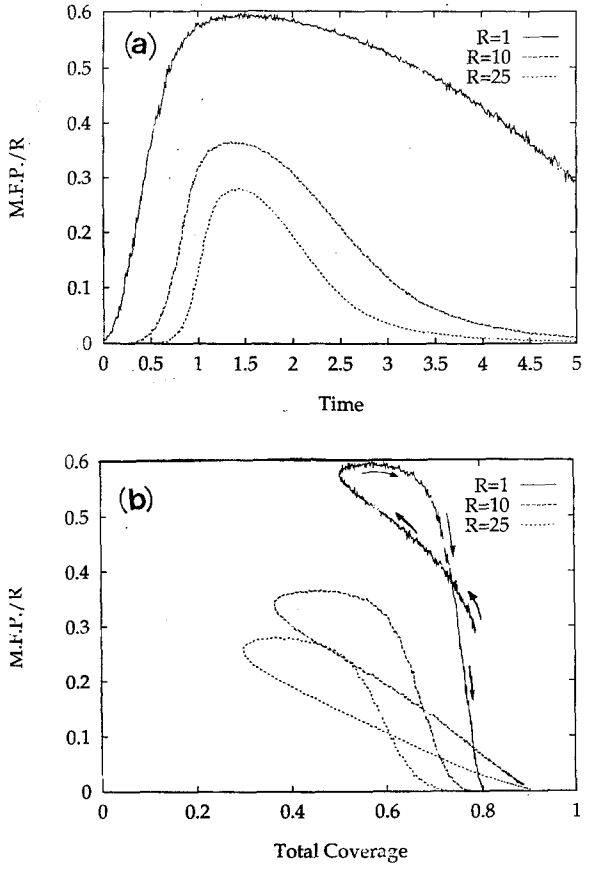

Fig. 11a, b. Plot of the average MFP of the "hot" monomers normalized with respect to R vs (**a**) time and (**b**) total surface coverage. In all cases one has $\theta_{A_0}=0.8$. Different choices of R are indicated in the figures. *Arrows* in **b** show the time direction

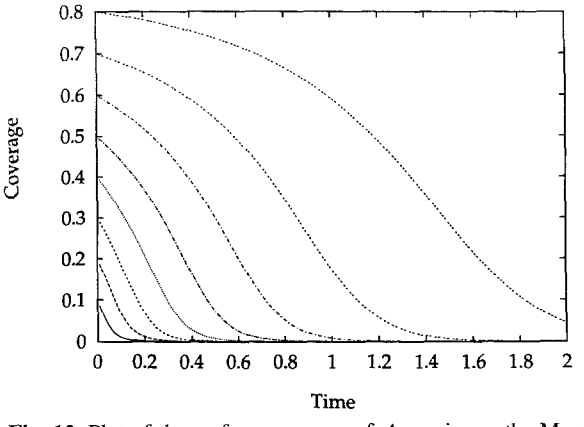

Fig. 12. Plot of the surface coverage of A-species vs the Monte-Carlo time for $R=25$ and different initial concentrations of preadsorbed A-species ($0.1 \leqq \theta_{A_0} \leqq 0.8$)

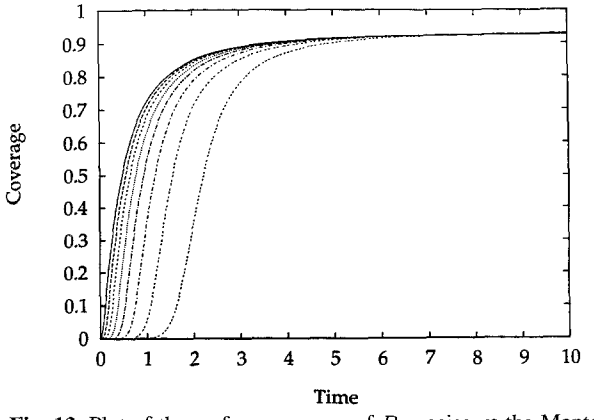

Fig. 13. Plot of the surface coverage of B-species vs the Monte-Carlo time for $R=25$ and different values of θ_{A_0}, ranging from $\theta_{A_0}=0.1$ (*left*) to $\theta_{A_0}=0.8$ (*right*), respectively

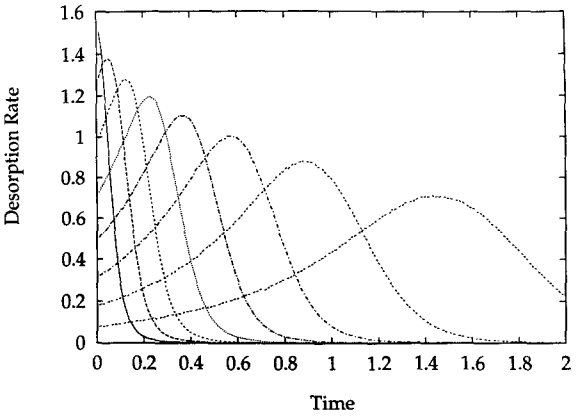

Fig. 14. Dependence of the desorption rate of the AB-product on time for $R=25$ and different values of θ_{A_0}, ranging from $\theta_{A_0}=0.1$ (*left*) to $\theta_{A_0}=0.8$ (*right*), respectively

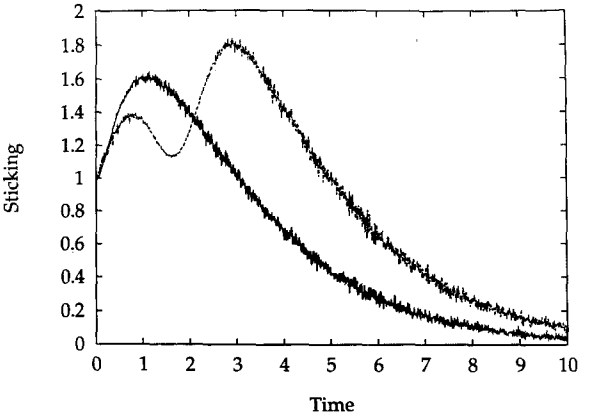

Fig. 15. Plots of the normalized sticking coefficient of "hot" dimers vs time for $R=25$ and $\theta_{A_0}=0.1$ (single peaked curve) and $\theta_{A_0}=0.8$ (double peaked curve), respectively

one observes, at early times, that when θ_{A_0} is increased almost all the "hot" species which become adsorbed can react and therefore $\theta_B \cong 0$ for $t \to 0$ (Fig. 13).

2.3.2 The Rate of AB-Production. Figure 14 shows the dependence of R_{AB} on t for $R=25$ and $0.1 \leqq \theta_{A_0} \leqq 0.8$. R_{AB} exhibits a peak which becomes broader and is shifted towards later times when θ_{A_0} is increased. This result agrees with Figs. 12 and 13, and reflects the fact that the removal of A-species from the surface is a slower process when θ_{A_0} increases.

2.3.3 The Sticking Coefficient of B_2-Species. Figure 15 shows plots of S/S_R versus t for $R=25$ taking $\theta_{A_0}=0.1$ and 0.8. The latter has also been plotted in Fig. 10 and exhibits two different regimes for $t<1.5$ and $T>1.5$, respectively, as it has already been discussed in Sect. 2.2.3. On the other hand, for $\theta_{A_0}=0.1$, one observes a single peak close to $t \cong 1$, which is characteristic of the B_2-adsorption kinetics [24], because A-species are already removed from the surface at early times ($t<0.2$).

2.3.4 The Mean Free Path of the "Hot" Monomers. For the sake of clarity plots of the MFP/R versus the total coverage are shown in Fig. 16a, for $0.1 \leqq \theta_{A_0} \leqq 0.4$, and Fig. 16b, for $0.5 \leqq \theta_{A_0} \leqq 0.8$, respectively. In Fig. 16a one observes that MFP/$R > 0$ for $t \to 0$ and $\theta_{A_0} \leqq 0.2$ since the A-coverage is rather small and then "hot" monomers can fly some distance over the surface before having encounters with B-species which leads to reaction. Nevertheless, for $\theta_{A_0} \geqq 0.3$ one has that MFP/$R \to 0$ for $t \to 0$ because "hot" dimers react almost immediately after desorption. In all cases, MFP/R increases when the total coverage decreases due to the $A+B$ reaction and reaches a maximum which depends on θ_{A_0}. After this maximum MFP/R decreases almost independently of θ_{A_0} (Fig. 16a). For $\theta_{A_0} \geqq 0.5$ (Fig. 16b) the behavior of MFP/R is somewhat more complicated since curves become flattened and peaks are broader than in the previous example (Fig. 16a). Nevertheless, the qualitative general behavior is similar in both cases shown in Fig. 16a, b, respectively.

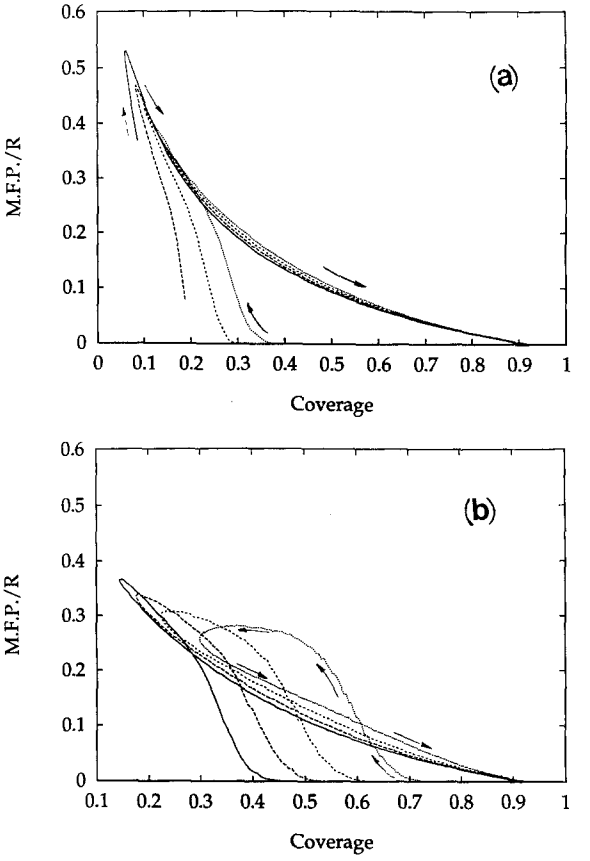

Fig. 16. a Plot of the average MFP of the "hot" monomers normalized with respect to $R=25$ vs the total surface coverage. Different values of θ_{A_0}, ranging from $\theta_{A_0}=0.1$ (left) to $\theta_{A_0}=0.4$ (right), respectively; **b** θ_{A_0} values ranging from $\theta_{A_0}=0.5$ (left) to $\theta_{A_0}=0.8$ (right), respectively. In both figures *arrows* show the time direction. More details in the text

3 Conclusions

A study of the surface reaction $A+(1/2)B_2 \to AB$ between "hot" B_2-dimers and preadsorbed A-monomers is presented. The study covers a wide spectrum of coverages of the preadsorbed species, namely $0.1 \leqq \theta_{A_0} \leqq 0.8$, as well as the range of R values ($0 \leqq R \leqq 100$) suggested by experi-

ments on the system O_2/Al(111) [17]. "Hot" dimers exhibit high efficiency for removal of preadsorbed species. As expected, this efficiency increases when increasing R. Consequently a remarkable enhancement of the rate of production of AB-species is observed due to the "hot"-dimer adsorption mechanism. This finding may be relevant in the dynamics of some catalyzed reactions such as, for example, the oxidation of carbon monoxide. The influence of the "hot"-dimer adsorption mechanism on the irreversible phase transitions of the dimer–monomer surface reaction scheme [7] is under progress. Preliminary results indicate that the critical points depend on R [27].

Acknowledgements. This work was financially supported by the CONICET, Argentina. The authors thank Prof. K. Binder, Institute of Physics, Johannes Gutenberg University of Mainz, for the warm hospitality during the preparation of the manuscript. Prof. G. Ertl, Fritz-Haber-Institute, DMG, Berlin, is greatly acknowledged for stimulating discussions. E.V.A. would like to acknowledge the Alexander von Humboldt Foundation (Germany) for the provision of a research fellowship.

References

1. R.B. Anderson, P.T. Dawson (eds.): *Experimental Methods in Catalytic Research,* Vols. I–III (Academic, New York 1976)
2. P.R. Norton: In Chemical Physics of Solid Surfaces and Heterogeneous Catalysis, ed. by D.A. King, D.P. Woodruff, Vol. 4 (Elsevier, Amsterdam 1982) p. 27
3. A.G. Sault, D.W. Goodman: In Model Studies of Surface Catlyzed Reactions, ed. by K.P. Lawley, Adv. Chem. Phys. (Wiley, New York 1989)
4. See, for example, the articles of various authors published in J. Stat. Phys. **42**, (1–2) (1986) which is devoted to overview recent progress in chemical kinetics
5. P. Fisher, U.M. Titulaer: Surf. Sci. **221**, 409 (1989)
6. C.H. Wu, E.W. Montroll: J. Stat. Phys. **30**, 537 (1983)
   L.W. Anacker, R. Kopelman, J.S. Whitehouse: J. Stat. Phys. **36**, 591 (1984)
   M. Silverberg, A. Ben-Shaul: J. Stat. Phys. **52**, 1179 (1988)
7. R.M. Ziff, E. Gulari, Y. Barshad: Phys. Rev. Lett. **56**, 2553 (1986)
8. P. Meakin, D.J. Scalapino: J. Chem. Phys. **87**, 731 (1987)
9. K. Fichthron, E. Gulari, R.M. Ziff: Phys. Rev. Lett. **63**, 1527 (1989)
10. M. Ehsasi, M. Matloch, O. Frank, J.H. Bloch, K. Chrismann, F.S. Rys, W. Hirschwald: J. Chem. Phys. **91**, 4949 (1989)
11. H.P. Kaukonen, R.M. Nieminen: J. Chem. Phys. **91**, 4380 (1989)
12. I. Jensen, H.C. Fogedby: Phys. Rev. A **42**, 1969 (1990)
13. E.V. Albano: J. Phys. A (Math. Gen.) **23**, L545 (1990)
14. E.V. Albano: Phys. Rev. B **42**, 10818 (1990)
15. E.V. Albano: Surf. Sci. **235**, 351 (1990)
16. E.V. Albano: J. Chem. Phys. **94**, 1499 (1991)
17. H. Brune, J. Wintterlin, R.J. Behm, G. Ertl: Phys. Rev. Lett. **68**, 624 (1992)
    H.-J. Güntherodt, R. Wiesendanger: Scanning Tunneling Microscopy I–III, Springer Ser. Surf. Sci., Vols. 20, 28, 29 (Springer, Berlin, Heidelberg 1992, 1993)
18. D.A. King, M.G. Wells: Proc. Royal Soc. (London) A **339**, 245 (1974)
19. N.O. Wolf, D.R. Burgess, D.K. Hoffman: Surf. Sci. **100**, 453 (1980)
20. J. Harris, B. Kasemo: Surf. Sci. **105**, L281 (1981)
    J. Harris, B. Kasemo, E. Törnqvist: Surf. Sci. **105**, L288 (1981)
21. S.L. Chang, P.A. Thiel: Phys. Rev. Lett. **59**, 296 (1987)
22. S.L. Chang, D.E. Sanders, J.W. Evans, P.A. Thiel: In *Structure of Surfaces II*, ed. by J.F. van der Veen, M.A. van Hove, Springer Ser. Surf. Sci., Vol. 11 (Springer, Berlin, Heidelberg 1988)
23. J.W. Evans: Rev. Mod. Phys. (1992) preprint
24. E. Albano, V. Pereyra: J. Chem. Phys. (1993), in press
25. J.W. Evans, D.R. Burgess, D.K. Hoffman: J. Chem. Phys. **79**, 5011 (1983)
26. J.W. Evans, R.S. Nord: Phys. Rev. B **31**, 1759 (1985)
    R.S. Nord, J.W. Evans: J. Chem. Phys. **93**, 8397 (1990)
27. V. Pereyra, E. Albano: In preparation